Transition Met Chem (2009) 34:899–904
DOI 10.1007/s11243-009-9279-8

Iron(III) Schiff base complexes with asymmetric tetradentate ligands: synthesis, spectroscopy, and antimicrobial properties

Lotf Ali Saghatforoush · Ali Aminkhani · Firoouzeh Chalabian

Received: 23 June 2009 / Accepted: 1 September 2009 / Published online: 25 September 2009

Abstract The synthesis and characterization is reported of four iron(III) complexes of general formula [Fe(pythsalX)-$(H_2O)_2$]Cl_2, derived from the NSNO-donor tetradentate Schiff base ligands pythsalHX ([5-X-N-(2-pyridylethylsulfanylethyl)salicylideneimine] (X = OMe, N_2Ph, I, NO_2). The complexes were characterized by physico-chemical and spectroscopic methods. The thermal stabilities of both the free Schiff bases and their complexes were studied by differential scanning calorimetry and thermogravimetric analyses. The spectroscopic data suggest that the Schiff base ligands coordinate through deprotonated phenolic oxygen, imine, and pyridine-type nitrogens and the thioether sulfur atoms to give an octahedral geometry around the iron(III) atom in all these complexes. The free Schiff bases and their complexes have been screened for antimicrobial activities and the results show that the free Schiff bases are more potent antibacterials than the complexes.

Introduction

Bioinorganic model chemistry has made extensive use of tetradentate ligands to mimic the active sites in metalloproteins and metalloenzymes [1, 2]. The design, synthesis, and characterization of iron complexes with Schiff base ligands has provided useful synthetic models for the iron-containing enzymes [3–5]. In particular, iron(III) complexes with salicylidene amine ligands provide a useful structural and electronic model for the similarly coordinated iron(III) sites found in the heme iron enzymes [6]. One of the most important characteristics of these Schiff base ligands is that even small modifications of the structure can significantly change key properties of the corresponding iron complex [3]. For example, the introduction of several electron-withdrawing nitro groups into iron complexes with salen-type ligands led to effective catalysts for hydrocarbon oxidation with dioxygen as the oxidant [7, 8]. It has been reported that the replacement of a methoxy group with an ethoxy group in a hexadentate N_4O_2 Shiff base ligand results in dramatic changes of the magnetic properties of the corresponding iron complexes, due to small alterations in the intermolecular interactions and crystal packing [9]. The recent discoveries of metal-sulfur and metal-nitrogen bonds at the active sites of several oxidoreductases such as hydrogenases, xanthine oxidase, and nitrogenase [10] have stimulated interest in pyridine and pyrimidine chemistry [10, 11] with mixed sulfur and nitrogen donor atoms. Synthesis, characterization, and reactivity studies of such complexes with N, S and N, S, O donor ligands can lead to valuable information toward understanding the functions of different enzymes at the molecular level [12].

In this investigation, we report on the synthesis, spectroscopic characterization, thermal properties, and antimicrobial activity of iron(III) complexes with monoanionic NSNO Schiff base ligands: [Fe(pythsalNO_2)$(H_2O)_2$]Cl_2, [Fe(pythsalOMe)$(H_2O)_2$]Cl_2, [Fe(pythsalN_2ph)$(H_2O)_2$]Cl_2, [Fe(pythsalI)$(H_2O)_2$]Cl_2. Although the synthesis of the

L. A. Saghatforoush (✉)
Department of Chemistry, Khoy Payam Noor University, Khoy, Iran
e-mail: saghatforoush@gmail.com

A. Aminkhani
Department of Chemistry, Islamic Azad University, Khoy Branch, Khoy, Iran

F. Chalabian
Department of Biology, Islamic Azad University, Tehran North Campus, Tehran, Iran

Schiff bases pythsalHX ([5-X-N-(2-pyridylethylsulfanylethyl) salicylideneimine] (X = OMe, N_2Ph, I, NO_2)) has been reported earlier [13], no research has been done so far on the iron complexes of these ligands.

Experimental

All chemicals and reagents used for the syntheses were commercial products (Merck or Fluka) and used without further purification. Solvents used for reactions were purified and dried by standard procedures [14]. 5-Iodosalcylaldehyde, 5-phenylazo-salcylaldehyde, and 1-(2-pyridyl)-3-thia-5amino pentane were synthesized according to known procedures [15–17]. 2-Vinylpyridine was distilled in vacuo before use. Elemental analyses (carbon, hydrogen, and nitrogen) were determined with an Elementar CHN Analyzer Vario El III. The molar conductance values of the complexes were measured in acetonitrile solution in room temperature with a Jenway 4510 conductometer instrument. Melting points were determined using an electrothermal apparatus and are uncorrected. The ^1H and ^{13}C NMR spectroscopic data were recorded on a Bruker spectrospin Avance 400 MHz in $CDCl_3$ and chemical shifts are indicated in ppm relative to tetramethylsilane. The electronic spectroscopic data in 200–900 nm range were recorded in acetonitrile on a Perkin-Elmer lambda 25 spectrophotometer. Infrared spectroscopic data (KBr disc, 4,000–400 cm^{-1}) were recorded on a Shimadzu FT-IR model prestige 21 spectrometer.

Antibacterial activity tests

The in vitro activity tests were carried out using the Growth Inhibitory zone (well method) [18, 19], against the four Gram-positive bacteria: *Streptococcus pyogenes*, *Streptococcus agalactiae*, *Staphylococcus aureus*, and *Bacillus anthracis* (RITCC 1036) and also against the two Gram-negative bacteria: *Klebsiella pneumoniae* (RITCC 1249) and *Pseudomonas aeruginosa (*RITCC 1547). Microorganisms (obtained from enrichment cultures of the microorganisms in 1 mL Muller–Hinton broth, incubated at 37 °C for 12 h) were cultured on Muller–Hinton agar medium. The inhibitory activities were compared with those of the standard antibiotic gentamicin (10 μg). After drilling wells in the medium using a 6 mm cork borer, 100 μL of solutions of the test compounds were poured into each well. The plates were incubated at 37 °C overnight. The diameter of the inhibition zone was measured to the nearest millimeter. Each test was carried out in triplicate and the average was calculated for inhibition zone diameters. A blank containing only methanol showed no inhibition in a preliminary test. The macro-dilution broth susceptibility assay was used for the evaluation of minimal inhibitory concentration (MIC). Twelve test tubes was used for the macro-dilution method. By including 1 mL Muller–Hinton broth in each test and then adding 1 mL extract with concentration 100 mg/mL in the first tube, we made serial dilutions of this extract from first tube to last tube. Bacterial suspensions were prepared to match the turbidity of 0.5 Mcfarland turbidity standards. Matching this turbidity provides a bacterial inoculum concentration of 1.5×10^8 cfu/mL. Then 1 mL of bacterial suspension was added to each test tube. After incubation at 37 °C for 24 h, the last tube in the series without turbidity was determined as the minimal inhibitory concentration (MIC).

Preparation of the Schiff bases

The four Schiff bases were synthesized in a similar manner [13]. A solution of 1-(2-pyridyl)-3-thia-5amino pentane (0.182 g, 1 mmol) in absolute ethanol (5 mL) was added to a solution of the required salicylaldehyde (1 mmol) in absolute ethanol (5 mL) to give clear yellow or light orange solutions. The mixture was refluxed for 1 h. Evaporation of the solution in vacuo gave viscous liquids. These were cooled in ice for 24 h to give microcrystals of the Schiff bases 5-X-N-(2-pyridylethylsulfanylethyl) salicylideneimine, where X = OMe, NO_2, I, N_2Ph. The microcrystals were filtered off, washed with cooled absolute ethanol, then recrystalized from ethanol–chloroform (2:1, v/v), and dried under vacuum.

5-Phenylazo-*N*-(2-pyridylethylsulfanylethyl) salicylideneimine, pythsalHN_2ph

Yield 0.254 g (65%), Anal. Found for $C_{22}H_{22}N_4OS$: C, 67.3; H, 5.8; N, 14.5%; Calcd: C, 67.7; H, 5.7; N, 14.3%; ^1H NMR (400 MHz $CDCl_3$) δ 13.80 (br s, 1H, OH), 8.39 (s, 1H, imine), [8.54 (d, $J = 4.5$ Hz, 1H), 7.98 (d, $J = 8.87$ Hz, 1H), 7.86–7.89 (m, 3H), 7.61(t, $J = 7.44$ Hz, 1H), 7.41–7.51 (m, 3H), 7.13–7.18 (m, 2H), 7.05 (d, $J = 8.87$ Hz, 1H) (total 12H ArH)], 3.80 (t, $J = 6.64$ Hz, 2H, $1 \times CH_2$), 3.08 (t, $J = 7.40$ Hz, 2H, $1 \times CH_2$), 2.98 (t, $J = 7.40$ Hz, 2H, $1 \times CH_2$), 2.85 (t, $J = 6.64$ Hz, 2H). ^{13}C NMR (400 MHz $CDCl_3$) δ 31.83, 32.94, 38.24, 58.38 (4C, aliphatic) 118.05, 118.27, 121.71, 122.53, 123.45, 126.96, 127.50, 129.09, 130.45, 136.77, 145.02, 149.12, 152.56, 159.54, 164.94, 165.67 (16C, aromatic). FTIR (KBr) ν 3400, 3069, 2850–2930, 1641, 1595 cm^{-1}. mp 140.8 °C. Red brown crystals.

5-Iodo-*N*-(2-pyridylethylsulfanylethyl) salicylideneimine, pythsalHI

Yield 0.289 g (70%), Anal. Found for $C_{16}H_{17}IN_2OS$: C, 46.7; H, 4.2; N, 6.8%; Calcd: C, 46.6; H, 4.1; N, 6.8%;

^{1}H NMR (400 MHz $CDCl_3$) δ 13.35 (br s, 1H, OH), 8.23 (s, 1H, iminic), [8.54 (d, $J = 4.82$ Hz, 1H), 7.64 (t, $J = 7.70$ Hz, 1H), 7.17–7.55 (m, 4H), 6.74 (d, $J = 8.53$ Hz, 1H) (total 7H, ArH)], [3.78 (t, $J = 6.64$ Hz. 2H, 1 × CH_2), 3.09 (t, $J = 7.20$ Hz, 2H, 1 × CH_2), 2.98 (t, $J = 7.20$ Hz, 2H, 1 × CH_2), 2.84 (t, $J = 6.64$, 2H, 1 × CH_2) (total 8H aliphatic)] ^{13}C NMR (400 MHz $CDCl_3$) δ 31.84, 32.97, 38.36, 58.93 (4C, aliphatic), 79.15, 119.57, 120.79, 121.60, 123.31, 136.52, 139.56, 140.68, 149.33, 159.67, 160.90, 164.55 (12C, aromatic). FTIR (KBr) ν 3485, 3053, 2853–2930, 1634, 1592 cm^{-1}. mp 62 °C. Yellow microcrystals.

5-Methoxy-*N*-(2-pyridylethylsulfanylethyl) salicylideneimine, pythsalHOMe

Yield 0.237 g (75%), Anal. Found for $C_{17}H_{20}N_2O_2S$: C, 64.0; H, 6.3; N, 8.7%; Calcd: C, 64.5; H, 6.4; N, 8.8%; ^{1}H NMR (400 MHz $CDCl_3$) δ 12.75 (br s, 1H, OH), 8.29 (s, 1H, iminic), [8.52 (d, $J = 4.44$ Hz, 1H), 7.58 (t, $J = 7.64$ Hz, 1H), 7.11–7.20 (m, 4H), 6.76 (d, $J = 8.1$ Hz, 1H) (total 7H ArH)], [3.81–3.75 (m, 1 × CH_2 and 1 × CH_3 methoxy group), 3.08 (t, $J = 7.36$ Hz, 2H, 1 × CH_2), 2.98 (t, $J = 7.36$ Hz, 2H, 1 × CH_2), 2.83 (t, $J = 6.80$ Hz, 2H, 1 × CH_2) (total 11H aliphatic)]. ^{13}C NMR (400 MHz $CDCl_3$) δ 31.90, 33.09, 38.44, 55.93, 59.33 (5C, aliphatic), 114.95, 117.23, 118.30, 119.38, 121.54, 123.27, 136.48, 149.29, 152.00, 155.21, 159.77, 165.55 (12C, aromatic). FTIR (KBr) ν 3447, 3053, 2850-2937, 1641, 1594 cm^{-1}. mp 54.7 °C. Orange microcrystals.

5-Nitro-*N*-(2-pyridylethylsulfanylethyl) salicylideneimine, pythsalHNO_2

Yield 0.258 g (78%), Found: C, 57.7; H, 5.2; N, 12.5%; Anal. Calcd for $C_{16}H_{17}N_3O_3S$: C, 58.0; H, 5.2; N, 12.7%; ^{1}H NMR (400 MHz $CDCl_3$) δ 14.55 (br s, 1H, OH), 8.35 (s, 1H, iminic), [8.55 (d, $J = 4.03$ Hz, 1H), 8.16-8.22 (m, 2H), 7.65 (t, $J = 7.64$ Hz, 1H), 7.19 (m, 2H), 6.96 (d, $J = 8.35$ Hz, 1H) (total 7H ArH)], [3.84 (t, $J = 6.5$ Hz, 2H, 1 × CH_2), 3.10 (t, $J = 7.28$ Hz, 2H, 1 × CH_2), 3.00 (t, $J = 7.28$ Hz, 2H, 1 × CH_2), 2.88 (t, $J = 6.5$ Hz, 2H, 1 × CH_2) (total 8H aliphatic)]. ^{13}C NMR (400 MHz $CDCl_3$) δ 31.70, 32.72, 38.21, 57.04 (4C, aliphatic), 116.65, 119.02, 121.69, 123.35, 128.21, 128.41, 136.62, 138.72, 149.25, 159.48, 164.98, 169.22 (12C, aromatic). FTIR (KBr) ν 3447, 3053, 2922-2940, 1655, 1594, 1325–1557 cm^{-1}. mp 96.3 °C. Orange microcrystals.

General synthesis of [Fe(pythsalX)$(H_2O)_2$]Cl_2 complexes

A solution of 1-(2-pyridyl)-3-thia-5-aminopentane (0.182 g, 1 mmol) in ethanol (5 mL) was added to the required salicylaldehyde (1 mmol) in ethanol (5 mL). The mixture was refluxed for 40 min and then 1 mL of 1 M methanolic NaOH was added, and reflux and stirring were continued for a further 5 min. A solution of $FeCl_3.6H_2O$ (0.27 g, 1 mmol) in ethanol 5 mL) was added with stirring and the reaction mixture was stirred under reflux for 50 min. The resultant colored solution was left at room temperature. The resulting precipitate was filtered off, washed with cold absolute ethanol, and recrystalized from methanol or acetonitrile and dried in vacuum.

5-Phenylazo-*N*-(2-pyridylethylsulfanylethylsal cylideneiminato κ^4N,N,O,S] iron(III) chloride dihyrate

Yield 0.35 g (63%), Anal. Found for $C_{22}H_{25}C_{l2}FeN_4O_3S$: C 47.2, H 4.5, N 10.0. Calcd: C 47.5, H 4.5, N 10.1. FTIR (KBr) ν 3447, 3080, 2920, 1623, 1445 cm^{-1}. UV (CH3CN) λ_{max}(nm) (ε lmol^{-1} cm^{-1}) 450 (143), 380 (30800), 255 (sh), 235 (20512). mp 199 °C dec. Mol. conductivity 233 μS. Light brown crystal.

5-Iodo-*N*-(2-pyridylethylsulfanylethylsal cylideneiminato κ^4 N,N,O,S] iron(III) chloride dihydrate

Yield 0.391 g (68%), Anal. Found for $C_{16}H_{20}Cl_2FeIN_2O_3S$: C 33.3, H 3.5, N 4.9. Calcd: C 33.5, H 3.5, N 4.9. FTIR (KBr) ν 3420, 3030–3080, 2870–2910, 1617, 1,444 cm^{-1}. mp 196 °C dec. UV (CH3CN) λ_{max}(nm) (ε lmol^{-1} cm^{-1}) 564 (143), 399 (4200), 325 (4550), 230 (28500). Mol. conductivity 198 μS. Dark red-brown crystals.

5-Methoxy-*N*-(2-pyridylethylsulfanylethylsal cylideneiminato κ^4 N,N,O,S] Iron(III) Chloride dihyrate

Yield 0.306 g (64%), Anal. Found for $C_{17}H_{23}Cl_2FeN_2O_4S$: C 43.1, H 4.8, N 5.8. Calcd: C 42.7, H 4.8, N 5.9. FTIR (KBr) ν 3425, 3070, 2840–2920, 1621, 1445 cm^{-1}. UV (CH3CN) λ_{max}(nm) (ε lmol^{-1} cm^{-1}) 568 (228), 360 (4225), 310 (4262), 258 (13830), 240 (13890). mp 173 °C dec. Mol. conductivity 215 μS. Dark red-brown crystals.

5-Nitro-*N*-(2-pyridylethylsulfanylethylsal cylideneiminato κ^4 N,N,O,S] Iron(III) Chloride dihyrate

Yield 0.196 g (59%), Anal. Found for $C_{16}H_{20}Cl_2FeN_3O_5S$: C 38.8, H 4.3, N 8.5. Calcd: C 39.0, H 4.1, N 8.5. FTIR (KBr) ν 3400, 3050–3120, 2830–2950, 1627, 1442, 1554, 1325 cm^{-1}. mp 201 °C dec. UV (CH3CN) λ_{max}(nm) (ε lmol^{-1} cm^{-1}) 508 (174), 350 (13100), 260(sh), 245 (15420). Mol. conductivity 196 μS. Dark brown crystals.

Results and discussion

Four tetradentate monoanionic ligands pythsalHX (X = N_2Ph, I, OMe, NO_2) all having an NSNO donor atom set were synthesized by the 1:1 condensation of the precursor 1-(2-pyridyl)-3-thia-5amino pentane with respective salicylaldehyde derivative in purified ethanol. Iron complexes of these ligands were obtained from a refluxing mixture of the respective Schiff base, methanolic NaOH, and hydrated iron(III) chloride, taken in a 1:1:1 molar proportion in ethanol (Scheme 1). The complexes were found to be fairly soluble in methanol, acetonitrile, DMF, and DMSO and display good stability in air at room temperature. Molar conductivities of all four complexes are in accord with 1:2 electrolyte behaviors [20]. The structures of the ligands were confirmed by ^{1}H and ^{13}C NMR spectroscopic data. In the ^{1}H NMR spectroscopic data of the free Schiff bases, no NH signal was found and it is therefore suggested that the Schiff bases do not undergo keto-enol tautomerism [21–23]. The spectrum of pythsalHOMe shows a signal at 59.33 ppm that can be attributed to the carbon atom of the methoxy group [23]. The FT-IR spectroscopic data of all the complexes compared with those of the free Schiff base show that the ν(C=N)$_{imine}$ band at 1,634–1,655 cm^{-1} is shifted to lower frequency by 17–28 cm^{-1} in the complexes, indicating that the ligands are coordinated to the metal atom through the nitrogen atom of the azomethine group [13]. The bands at 1,592–1,595 cm^{-1} due to ν(C=N)$_{py}$ in the free Schiff bases appear at 1,442–1,445 cm^{-1} in the complexes [21, 22]. The absence of the OH bands of the Schiff bases from the spectra of the complexes indicates that the OH group has been deprotonated and coordinates to the metal as O^-. A relatively medium broad absorption band with maximum at 3,400–3,450 cm^{-1} indicates the presence of water and the elemental analyses the complexes show the presence of two moles of water in one mole of the complexes. The spectroscopic data of the pythsalHNO$_2$ ligand and its complex show two bands at 1,325–1,557 cm^{-1} and these can be attributed to ν(NO_2) of the nitro group [23].

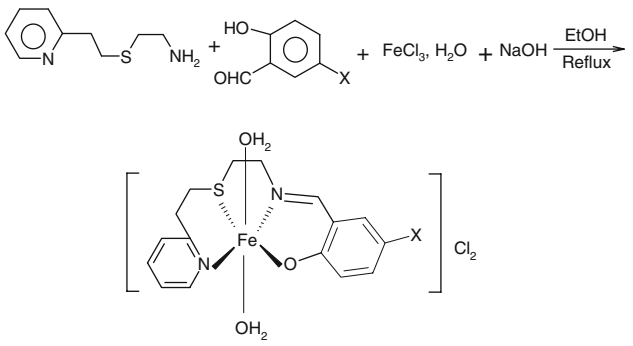

Scheme 1 Preparation of the complexes. X = I, NO_2, OMe, N_2Ph

The electronic spectra of the complexes were measured in acetonitrile solution. In general, the electronic transitions for iron(III) systems are spin forbidden and hence weak, and are often masked by charge transfer bands [24]. However, in several spin equilibrium systems, the high spin (S = 5/2) form has been characterized by a transition at 555–500 nm and the low spin (S = 1/2) form by a transition at ~714–625 nm [24–26]. From the spectra of these iron(III) complexes, it can be seen that all of them exhibit one band at 508–568 nm which can be assigned to the $^6A_{1g} \rightarrow {}^4T_{1g}$ transition characteristic of octahedral structure [24, 27, 32]. The maximum of the d–d ligand field band is shifted from 508 nm in [Fe(pythsalNO_2)(H_2O)$_2$]Cl_2 to 568 nm in [Fe(pythsalOMe)(H_2O)$_2$]Cl_2. This behavior reflects changes in Lewis acidity of the iron(III) center due to the presence of the OCH_3 donating group in pythsalHOMe which decreases the degree of any iron to ligand bonding [3]. As noted above, the d-d band in [Fe(pythsalN_2ph)(H_2O)$_2$]Cl_2 may be masked by charge transfer bands [24]. The broad, intense and poorly resolved bands between 320–450 nm may be assigned to LMCT or MLCT [28–30]. The high intensity band below 320 nm may be assigned to intraligand n–π*/π–π* transition [31, 32].

Thermal studies of the Schiff base and their iron complexes were performed using DSC and TGA. Enthalpy changes and decomposition temperatures are tabulated in Table 1.

DSC studies of the free Schiff bases showed melting, followed by exothermic decomposition. Among the free Schiff bases, pythsalHOMe has the greatest stability. DSC data for the iron complexes show that [Fe(pythsalI)(H_2O)$_2$]Cl_2 decomposes before melting, at 209 °C. [Fe(pythsalOMe)(H_2O)$_2$]Cl_2, [Fe(pythsalNO_2)(H_2O)$_2$]Cl_2 and [Fe(pythsalN_2ph)(H_2O)$_2$]Cl_2 all melt before undergoing exothermic decomposition. The water contents were studied by thermal

Table 1 Transition temperatures, enthalpy changes and decomposition temperatures of free Schiff base ligands and related Fe(III) complexes

Compound	$T^{a,b}$ (°C)	ΔH^a (kJ mol^{-1})	T_d^c (°C)
pythsalHI	62.2 (mp)	−31.5	221
pythsalHOMe	54.7 (mp)	−26.7	279
pythsalHNO_2	96.3 (mp)	−42.5	238
pythsalHN_2Ph	140.8 (mp)	−27.1	253
[Fe(pythsalI)(H_2O)$_2$]Cl_2	209.4 (dec)	111.0	210
[Fe(pythsalOMe)(H_2O)$_2$]Cl_2	173.8 (mp)	−28.4	231
[Fe(pythsalNO2)(H_2O)$_2$]Cl_2	200.6 (mp)	−20.3	235
[Fe(pythsalN2ph)(H_2O)$_2$]Cl_2	181.2 (mp)	−33.9	218

[a] Data obtained from first DSC cycle

[b] *dec* decomposed, *mp* melting point

[c] Data obtained from TGA; 10 °C min^{-1} under N_2 gas

Table 2 Thermoanalytical results (TGA) of Fe(III) Schiff base complexes

Complex	Decomposition	T (°C)	Lost species	Weight loss	
				Calculated	Found
$[Fe(pythsalI)(H_2O)_2]Cl_2$	First step	127	$2H_2O$	6.3	6.0
	Second step	210	pythsalI	71.6	70.5
$[Fe(pythsalOMe)(H_2O)_2]Cl_2$	First step	130	$2H_2O$	7.5	7.8
	Second step	231	pythsalOMe	66.0	65.8
$[Fe(pythsalNO2)(H_2O)_2]Cl_2$	First step	134	$2H_2O$	7.2	7.7
	Second step	235	$pythsalNO_2$	67.0	66.3
$[Fe(pythsalN_2ph)(H_2O)_2]Cl_2$	First step	135	$2H_2O$	6.5	6.7
	Second step	218	$pythsalN_2Ph$	70.2	70.5

analysis. The temperature values for the decomposition and the species lost in each step of the decomposition reactions of the iron(III) complexes are given in Table 2. The data are consistent with the proposed formulae and indicate that all of the complexes undergo two-step degradation reactions. The first step occurs at a maximum lying in the region above 127 °C. The weight loss in this step agrees with the loss of two water molecules [33]. The last step in the degradation of the complexes occurs in the region around 210 °C and might be associated with the loss of the ligand. Of these complexes, $[Fe(pythsalNO_2)(H_2O)_2]Cl_2$ has highest thermal stability and the order of thermal stability of the complexes is not the same as that for the free Schiff bases. The final decomposition product was iron oxide as confirmed by qualitative analysis.

The antibacterial activities (zones of growth inhibition and minimal inhibitory concentrations) of three Schiff bases, their iron(III) complexes and gentamicin (as a standard compound) are shown in Table 3. The organisms used in the present investigation included *Streptococcus pyogenes* (RITCC 1940), *Streptococcus agalactiae* (RITCC 1913), *Staphylococcus aureus* (RITCC 1885), and *Bacillus anthracis* (RITCC 1036) as gram-positive bacteria and *Klebsiella pneumonia* (RITCC 1249) and *Pseudomonas aeruginosa* (RITCC 1547) as gram-negative bacteria. The data indicate high activity of pythsalHI Schiff base against both the gram-positive bacteria and the two gram-negative bacteria. The other Schiff bases show variable activities. The significant activities of the Schiff bases may arise from the presence of imine, hydroxyl, and pyridyl-N functional groups [36–38]. pythsalHI was the most potent antibacterial agent, indicating that the iodine plays an important role in the antibacterial activity [34, 35]. The three iron(III) complexes that were tested have moderate activity (inhibitory zones >15 mm) against all four gram-positive bacteria, except $[Fe(pythsalNO_2)(H_2O)_2]Cl_2$ that has weak activity toward *S. aureus* [39]. Also the results in Table 3, indicate that the all three complexes are moderately active against the two gram-negative bacteria (inhibitory zones >15 mm), except for $[Fe(pythsalNO_2)(H_2O)_2]Cl_2$ which shows weak activity toward *pneumoniae* [39].

Table 3 Minimum inhibitory concentration (mg/mL) (MIC)

Method	Main compounds	Microorganism					
		pyogenes	*agalactiae*	*aureus*	*anthrcis*	*pneumonia*	*aeruginosa*
Growth inhibitory zone (mm)	pythsalHI	40	46	42	50	26	18
	$pythsalHNO_2$	40	30	20	20	20	20
	pythsalHOMe	40	20	10	20	20	10
	$[Fe(pythsalI)]Cl_2$	16	20	15	30	20	20
	$[Fe(pythsalNO_2)]Cl_2$	25	15	10	20	5	15
	$[Fe(pythsalOMe)]Cl_2$	20	20	30	25	15	15
	Gentamicine	20	–	20	32	20	16
MIC	pythsalHI	6.2	3.2	6.2	3.2	12.2	25
	$pythsalHNO_2$	6.2	12.5	25	25	25	25
	pythsalHOMe	6.2	25	50	25	25	50
	$[Fe(pythsalI)]Cl_2$	50	25	25	12.5	25	25
	$[Fe(pythsalNO_2)]Cl_2$	18.7	37.5	50	25	100	37.5
	$[Fe(pythsalOMe)]Cl_2$	25	25	12.5	18.7	37.5	37.5

The antibacterial activities for the complexes are lower than those found for the free Schiff bases, except $[Fe(pythsalOMe)(H_2O)_2]Cl_2$ which shows strong to moderate activity against *aureus, anthracis*, and *aeruginosa* compared to free pythsalHOMe.

Conclusion

We have prepared iron(III) complexes of four Schiff base ligands and characterized them by physico-chemical and spectroscopic means. They are formulated as 1:2 electrolytes of general formula $[Fe(pythsalX)(H_2O)_2Cl_2$. The infrared spectra reveal a common mode of complexation through the nitrogen atoms of the azomethine and pyridine groups, oxygen atom of deprotonated phenolic group and thioether sulfur atom. Thermal analyses data show good agreement with the suggested formulae. The electronic spectra indicate octahedral geometry for the complexes. The parent Schiff bases proved to be more potent antibacterials than their iron(III) complexes.

Acknowledgement We thank the research Office of Payam Noor University for supporting this work.

References

1. Heistand RH II, Lauffer RB, Fikrig E, Que L Jr (1982) J Am Chem Soc 104:2789
2. Mukherjee RN, Abrahamson AJ, Patterson GS, Stack TDP, Holm RH (1988) Inorg Chem 27:2137
3. Kannappan R, Tanasae S, Mutikainen I, Turpeinen U, Reedijk J (2006) Polyhedron 25:1646
4. Sivasubramanian VK, Ganesan M, Rajagopal S, Ramaraj R (2002) J Org Chem 67:1506
5. Fujii H, Kurahashi T, Ogura T (2003) J Inorg Biochem 96:133
6. Canali L, Sherrington DC (1999) Chem Soc Rev 28:85
7. Bottcher A, Grinstaff MW, Labinger JA, Gray HB (1996) J Mol Catal A – Chem 113:191
8. Bottcher A, Birnbaum ER, Day MW, Gray HB, Grinstaff MW, Labinger JA (1997) J Mol Catal A–Chem 117:229
9. Salmon L, Bousseksou A, Donnadieu B, Tuchagues JP (2005) Inorg Chem 44:1763
10. Roy S, Mandal TN, Barik AK, Pal S, Gupta S, Hazra A, Butcher RJ, Hunter AD, Zeller M, Kar SK (2007) Polyhedron 26:2603
11. Muller A, Krebs B (eds) (1984) Sulfur, its significance for chemistry, for the geo- and cosmosphere and technology, studies in inorganic chemistry, vol 5. Elsevier Science Publishers, Amsterdam
12. Llort F, De Munno G, Julve M, Cano J, Ruiz R, Caneschi (1998) Angew Chem Int Ed 37:135
13. Daneshvar N, Entezami AA, Khandar AA, Saghatforoush LA (2003) Polyhedron 22:1437
14. Perrin DD, Armarego WLF (1980) Purification of laboratory chemicals, 3rd ed. Pergamon, Oxford, pp 68, 174, 217
15. Pavia RM, Cohen PM, Dilley JC, Dubuc RG, Duginal LT, Forman WF, Hediger EM, Milota G, Powers ST, Sucholeiki I, Zhou S, Hangauer GD (1996) Biorg Med Chem 4:659
16. Khandar AA, Rezvani Z (1998) Polyhedron 18:129
17. Kaasjager VE, Puglisi L, Bouwman E, Driessen WL, Reedijk J (2000) Inorg Chem Acta 310:183
18. Baver A, Kirby WMM, Sherris JE, Turck M (1986) Am J Clin Pathol 45:493–496
19. Indu1 MN, Hatha AAM, Abirosh C, Harsha U, Vivekanandan G (2006) Braz J Microbiol 37:153–158
20. Szafran Z, Pike RM, Singh MM (1991) Microscale inorganic chemistry. Wiley, New York, p 104
21. Tumer M, Erdogan B, Koksal H, Serin S, Nutku Y (1998) Syn React Inorg Met Org Chem 28:529
22. Keypour H, Dehghani-Firouzabadi AA, Khavasi HR (2009) Polyhedron 28:1546
23. Williams DH, Fleming I (1989) Spectroscopic methods in organic chemistry, 4th ed. McGraw Hill, London, pp 52–54, 73, 135
24. Sarkar S, Dey K (2005) Spectrochim Acta A 62:383
25. Dose EV, Murphy KMM, Wilson LJ (1976) Inorg Chem 15:2622
26. Maeda Y, Tsutsumi N, Yakashima Y (1984) Inorg Chem 23:2440
27. Gaber M, Issa RM, Ghoniem MM, El-Baradie KY (1991) Egypt J Chem 34:107
28. Atkins R, Brewer G, Kokot E, Mockler GM, Sinn E (1985) Inorg Chem 24:134
29. Lever ABP (1984) Inorganic electronic spectroscopy, 2nd edn. Elsevier, Amsterdam, pp 450–451
30. Garica AS, Albertin JP, Collet A, Faury L, Pastor JM, Tosil L (1981) J Chem Soc Dalton Trans 2544
31. Rahman SkH, Chowdhury H, Bose D, Ghosh R, Hung CH, Kumar Ghosh B (2005) Polyhedron 24:1755
32. Madha NT, Radhakrishnan PK, Grunert M, Weinberger P, Linert W (2003) Thermochim Acta 407:73
33. El-Behery M, El-Twigry H (2007) Spectrochim Acta A 66:28
34. Shi L, Ge HM, Tan SH, Li HQ, Song YC, Zhu HL, Tan RX (2007) Eur J Med Chem 42:558–564
35. Lv J, Liu T, Cai S, Wang X, Lu L, Wang Y (2006) J Inorg Biochem 100:1888–1896
36. Mohamed GG, Abd El-Wahab ZH (2005) Spectrochim Acta A 61:1059–1068
37. Sari N, Arsalan S, Logoglu E, Sakiyan I (2003) J Sci 16:283–288
38. Zidan ASA (2003) Phosphorus Sulfur Silicon 178:567–582
39. Chew K-B, Tarafder MTH, Crouse KA, Ali AM, Yamin BM, Fun H–K (2004) Polyhedron 23:1385–1392